

Analysis of Radiation Pattern and Beamforming in Phased Antenna Arrays for Indoor Localization and Scanning Systems

Octavian Manu¹, Mihai Dimian¹, Anneleen Van Nieuwenhuysse², Adrian Graur¹

¹Electrical Engineering and Computer Science Department – Ştefan cel Mare University Suceava, RO

²Department of Industrial Engineering/Electronics – Catholic University College Ghent, BE

Corresponding address: dimian@eed.usv.ro

Abstract — This paper presents an analysis of radiation pattern and beamforming in phased antenna arrays for indoor localization and scanning based on a triangulation technique. Beamforming is obtained and steered by applying a linear phase shift between antenna array elements, which provides a simple and power efficient design. Various antenna array configurations are studied by numerical simulation means in order to obtain an optimal beamforming necessary for indoor localization and scanning systems in wireless sensor network.

Index Terms — Phased Antenna Array, Indoor localization, Beamforming, Radiation Pattern Simulation

I. INTRODUCTION

The indoor localization and scanning have received an increasing amount of research interest over the last years due to their great potential for various applications [1, 2]. The traditional use of indoor localization ranges from tracking a specific object to helping someone in finding the way around an unfamiliar building. Hospitals and day care centers have recently started using positioning technologies to locate personnel or medical equipment in case of an emergency. A rapidly development field for applying indoor localization is in the area of smart sensor networks where data recorded from a wireless sensor are correlated to their position. Other promising applications are related to shopping assistance and follow-me services.

The localization procedure is performed by using trilateration technique involving time of arrival (TOA) or received signal strength (RSS), multilateration technique involving time difference of arrival (TDOA) or triangulation technique involving angle of arrival (AOA). In the case of TOA, a sphere of presence can be estimated by acquiring the time of flight and multiplying it with the light speed. In the case of RSS, the distance is computed from the power path loss by measuring the received power and comparing it with the transmitted power. Consequently, the position of the user can be obtained from the intersections of three or more spheres of presence, which concludes the trilateration method. By measuring TDOA of a signal from the emitter at two receivers a hyperboloid surface of possible locations is determined, so four or more receivers can uniquely determine the emitter location as the intersection of three hyperboloids, which constitutes the multilateration method. The third method of localization, triangulation, uses the baseline and at least two AOA. However, the possible absence of the line of sight, multi-path diversity along with other wave-related phenomena significantly increase the degree of complexity for the indoor localization and scanning regardless of the technique used and the measurement accuracy [3, 4].

In terms of practical implementation, various technologies, such as GPS, RFID, GSM or W-LAN, have been employed in building the indoor localization and scanning systems, but no definite solution currently exists [1, 5].

II. BEAMFORMING

The analysis performed in this paper is related to indoor localization and scanning based on a triangulation technique which involves smart antennas for measuring of angle of arrival. Smart antennas are capable of electronically modifying its radiation pattern and can be realized by using an array of linear antenna elements equipped with variable phase shifters or time delays. In addition, signal processing techniques, coined as beamforming, can be used in antenna array for directional signal transmission or reception. The desired radiation pattern consists of a main lobe which is as narrow as possible and significantly longer than the sidelobes. An electronically steered array used for localization purposes can be practically realized either as a switched beams array or as an adaptive antenna array. In the case of switched beams array, antenna switches periodically between the predefined beams pattern in order to cover the scanning plane. The beam must have a sufficient number of steps in order to efficiently cover the scanning plane. When transmitting, a beam former controls the phase and/or relative amplitude of the signal at each transmitter, in order to create a pattern of constructive and destructive interference in the wave front. The adaptive array system can offer optimal gain since it actively identifies and tracks both the desired and the interfering signals. The capability for active interference offers the adaptive systems major advantages and flexibility over the more passive switched beam approaches.

III. THEORETICAL APPROACH

Let us consider an antenna array with K linear elements oriented along z -axis (see Fig. 1) with a linear phase taper between antenna elements of ψ_i . The total signal received by the antenna array in the horizontal plane at angle φ with y -axis (normal to the array) can be written as follows [6]:

$$S(\varphi) = S_e(\varphi) \cdot S_a(\varphi) \quad (1)$$

where $S_e(\varphi)$ represents the complex radiation pattern of one individual radiator and $S_a(\varphi)$ is known as the array factor and is explicitly given by the following formula:

$$S_a(\varphi) = \sum_{i=1}^K e^{j[k_0(K-i)d \sin(\varphi) + \psi_i]} \quad (2)$$

where k_0 represents the free space wavenumber, while d is the spacing between antenna elements.

In order to form a beam in the desired direction φ_0 let us choose a linear phase taper of the following form:

$$\psi_i = -k_0(K-i)d \sin(\varphi_0) \quad \text{for } i = 1, 2, \dots, K, \quad (3)$$

The maximum of the corresponding array factor is attained for: $\sin(\varphi) - \sin(\varphi_0) = 0$, or, provided that $-90^\circ \leq \varphi, \varphi_0 \leq 90^\circ$, for $\varphi = \varphi_0$. Thus, by choosing a desired beam-pointing direction φ_0 and subsequently phasing the linear antenna array elements according to $\psi_i = -k_0(K-i)d \sin(\varphi_0)$, the array factor will reach its maximum at the desired angle $\varphi = \varphi_0$. This property can be used to design the phased antenna array for indoor scanning and localization.

However, the previous theoretical analysis has not taken into consideration the mutual coupling between antenna elements nor the interaction between the radiation and the indoor environment. Parts of these issues are addressed in section IV.

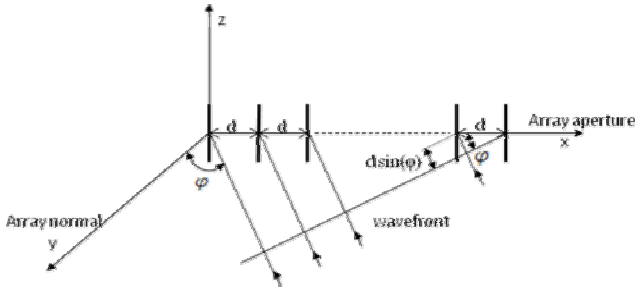


Fig. 1. Schematic representation of the linear antenna array and the coordinate axes.

Next, let us address the problem of feeding networks for phased arrays. There exist various solutions to feed the array elements in order to form the desired beam pattern [7], both parallel and series feeds being considered. **Error! Reference source not found.** depicts two types of feed networks that include a main transmission line from which energy is tapped to feed the radiating elements. Steering the beam in the desired direction is accomplished by adding phase shifters in either of the branch line feeding the elements or in the main line. Both designs excel in construction simplicity and are capable of handling full waveguide power at the input. However the control of the series feed configuration is simpler than the parallel one due to the identical phase shifts used by all phase shifters for a given steering angle, but it is less power efficient by cumulating the losses from each array element.

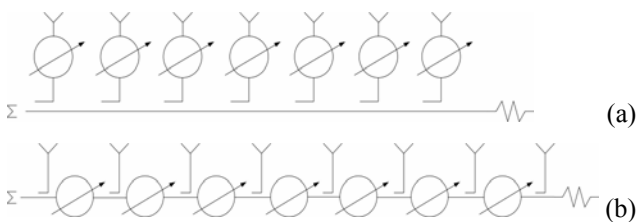


Fig. 2. (a) Parallel feed network, (b) Series feed network.

IV. TWO-ELEMENT ANTENNA ARRAY

Antenna array simulations were performed by using 4NEC2 software which is a freeware software package based on Numerical Electromagnetic Code version 2 (NEC2) developed at Lawrence Livermore National Laboratories by G. J. Burke and A. J. Poggio. NEC2 computes the numerical solution of integral equations for induced currents and simulates the electromagnetic response of antennas and metallic structures by using Method of Moments.

In the first part of our analysis, numerous numerical simulations have been performed for various geometrical configurations of antenna array and different phase shift between elements and the results were compared with the corresponding analytical calculations based on Eqs. 2 & 3. Since 4NEC2 software takes into account the mutual coupling between antennas elements neglected in the derivation of Eq. 2, this comparison provides a clear account of the electromagnetic coupling influence on the array radiation pattern. The results of this comparison for the normalized array factor pattern of a 2 elements linear antenna array with half wavelength spacing are presented in Fig. 3 for phase shifts corresponding to steering angle φ_0 equal to 0° , 45° and 90° . It is apparent that the mutual coupling effect on the radiation pattern is negligible for broad-side ($\varphi_0=0^\circ$) and end-fire ($\varphi_0=90^\circ$) configurations, but it is significant for intermediate phase shifts.

Experimental setup used for measuring the radiation pattern of antenna array is presented in Fig. 4 and consists of Data Acquisition interface / Power Supply and Antenna Positioner connected to the antenna array and RF Generator connected to a Yagi-Uda antenna, which are parts of LAB-VOLT Antenna Training and Measuring System. Two monopole antennas were placed on two masts on antenna positioner at a distance of half lambda between them. By using data acquisition interface, antenna positioner was controlled to rotate uniformly by 360 degree and the received power level was measured at each degree.

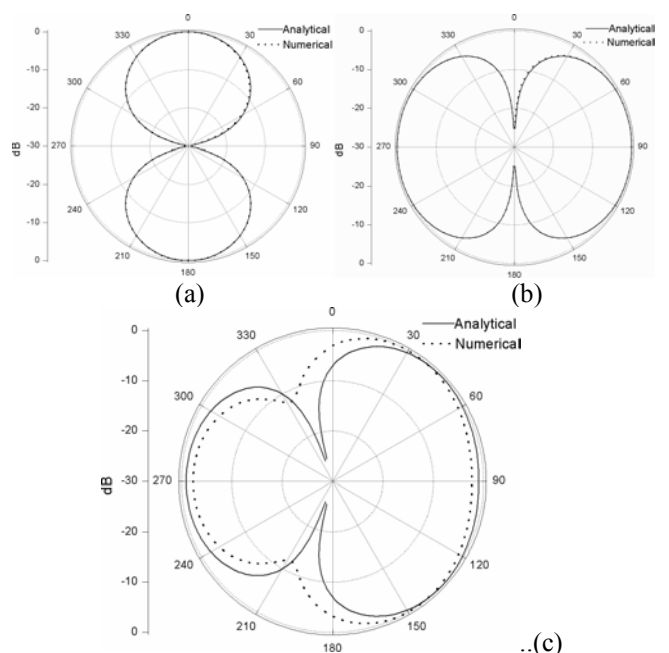


Fig. 3. Analytical and numerical radiation pattern of a 2 elements array with φ_0 equal to (a) 0° , (b) 90° , (c) 45° .



Fig. 4. Radio Frequency Generator – left and Antenna Positioner connected to Data Acquisition Interface – right.

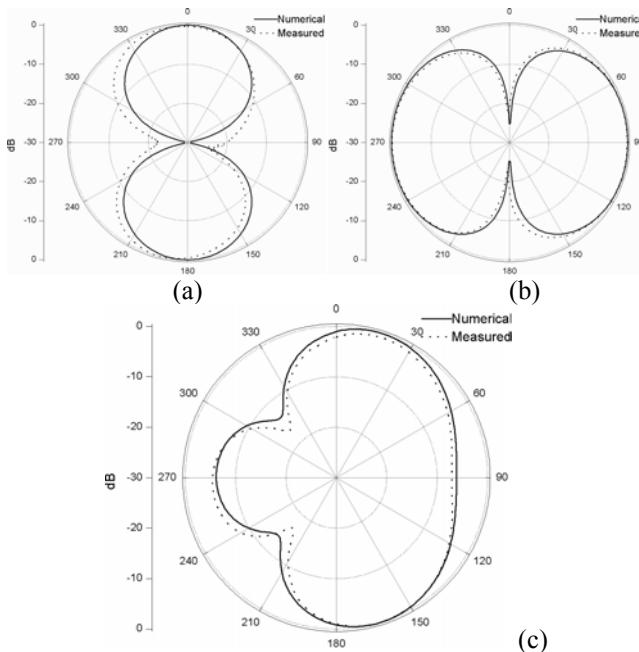


Fig. 5. Numerical and measured radiation pattern of a 2 elements array with φ_0 equal to (a) 0° , (b) 90° , (c) 30° .

The connection between antennas and the data acquisition module was done via a signal summing/splitter using coaxial cables with 50ohms impedance and a speed of 66% light speed. The transmitter frequency was set to 915MHz.

In the first set of experiments, two coaxial cables of 30cm length have been used for connecting the antenna elements to the summing/splitter, which resulted in no phase difference between antenna elements. In order to obtain a phase shift of 90° (corresponding to $\varphi_0=30^\circ$), a second set of experiments were performed that used a connecting cable of 30cm for one element and a cable of 35.4 cm for the other. The difference of 5.4 cm corresponds to a quarter wavelength taking into account the signal speed in the connecting cables and the operating frequency. The last set of measurements were performed for a phase shift between antenna elements of 180° (corresponding to $\varphi_0=90^\circ$) realized by using one cable of 30 cm and one of 40.8 cm, where the 10.8 cm difference represents half of wavelength. The radiation patterns have been measured in the plane perpendicular to the antenna array (H-plane), where each individual monopole antenna features an isotropic

radiation. Samples of experimental results from each set of measurements and the corresponding numerical simulations are presented in Fig. 5.

The measured radiation pattern resembles the simulation results, while the differences between the simulation and measurements can be interpreted as the influence of the environmental conditions (wall reflections, misalignments, deviation from the far-field approximation considered in the theory, etc.), as well as the inherent experimental errors which are considered to be of the order of 2% in our experimental set-up. In conclusion, the numerical simulations are in good agreement with the analytical and experimental results. They provide important corrections to the analytical calculations by taking into account the electromagnetic coupling between antenna elements and offer a better image of the environmental influence and experimental errors that generally affect the radiation measurements.

As it is apparent from Figs. 3 and 5, by superposing of the radiations from two antennas with isotropic radiation in H-plane, separated by a half-wavelength distance, one can obtain a directional radiation pattern with two major lobes oriented along y-axis for 0 phase shift. The radiation pattern can be rotated with 90° , though the two-lobes are also enlarged, by applying an 180° phase shift between the two elements. Unfortunately, the intermediate phase shifts do not lead to a coherent rotation of this directional radiation pattern in the scanning plane, as one can see in the snapshot presented in Fig. 5 (c). In order to obtain narrower lobes and coherent lobe rotation, phased antenna arrays with higher number of elements are next addressed.

V. MULTI ELEMENTS ANTENNA ARRAY

In this study, numerous linear antenna arrays consisting of 6, 8 and 12 antenna elements with various phase tapers between antenna elements have been simulated and analyzed. It has been observed that the beamwidth of the major lobes is decreasing by increasing the number of elements and is increasing with scanning angle, the minimum beamwidth being obtained in broadside array configuration while the maximum beamwidth is achieved in an end-fire array configuration.

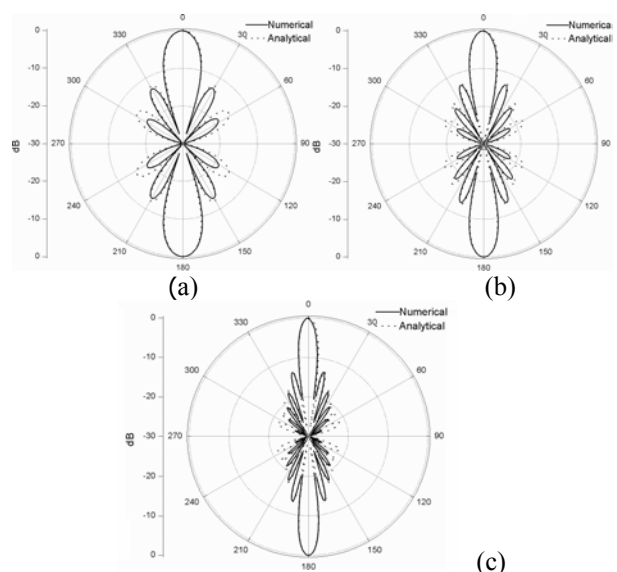


Fig. 6. Radiations pattern of a (a) 6, (b) 8 and (c) 12 elements antenna array with φ_0 equal to 0° .

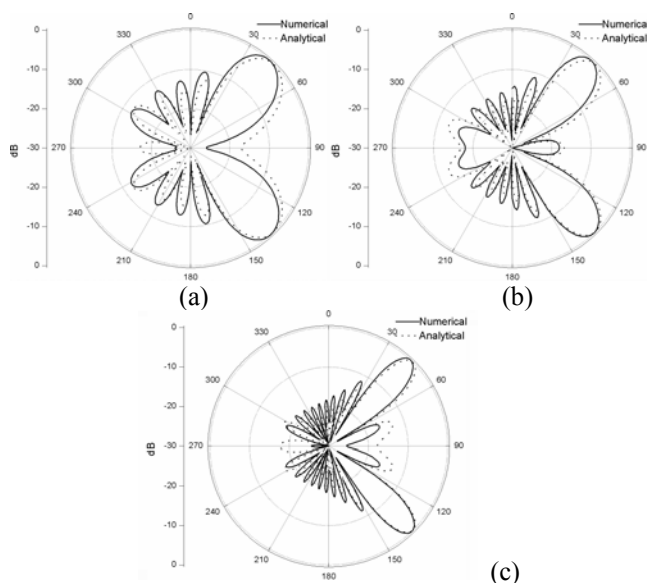


Fig. 7. Radiation pattern of a (a) 6, (b), 8, and (c) 12 elements antenna array with φ_0 equal to 45° .

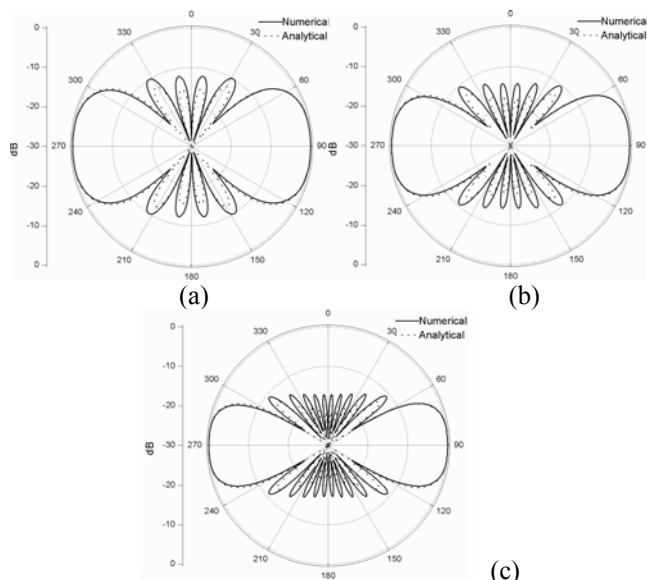


Fig. 8. Radiations pattern of a (a) 6, (b) 8, and (c) 12 elements antenna array with φ_0 equal to 90° .

These conclusions are apparent from the sample results for the corresponding radiation patterns presented in Figures 6, 7 and 8 (simulation results using 4NEC2 are plotted by continuous lines and the analytical results obtained by neglecting the antenna element coupling are plotted by dotted lines). In broadband array configuration presented in Figure 6, the beamwidth of the major lobes is 16° for 6-elements antenna, 12° for the 8-elements antenna, and 8° for 12 elements antenna, while the other two figures show a significant increase of the major lobe beamwidth with the scanning angle.

VI. CONCLUSIONS

Beamforming techniques have been usually applied in military applications, and more recently in base stations for telecommunication. Despite of many potential advantages, its applications in consumer electronics are scarce due to relatively high cost of the current implementations. Thus, the typical implementation of beamforming uses special-

ized microwave and radio frequency (RF) technologies with hybrid module assembly techniques, and many RF-cables and connectors, unsuitable for cost-effective mass production. The presented simulations have shown that it is possible to implement beamforming in antenna array by using phase taper only. This method could be used for triangulation localization in wireless sensor network (WSN) where are clear limitations for power consumption, fabrication cost and device complexity.

The case of two element antenna array has been first analyzed in order to compare the numerical simulations with known analytical results and with experimental measurements performed in our laboratory. While a good agreement was observed in both analytical and experimental comparisons, the numerical simulations have also provided important corrections to the analytical calculations by taking into account the electromagnetic coupling between antenna elements and offered a better image of the environmental influence and experimental errors reflected in the radiation measurements. However, the resulting radiation patterns have major lobes that can be considered too broad and do not perform a coherence rotation when increasing the phase shift, which make them less suitable for indoor localization and scanning systems.

In order to obtain better results the number of elements of the antenna array should be increased. Thus, the beamwidth of the major lobes decreases, providing the possibility to do a more precise localization, and an approximate coherent rotation of the major lobes is observed by changing the phase shift. However, a special attention should be paid to the side lobes whose number increases with the number of antenna elements. Thus, it is recommended to have the scanning area covered by at least two antenna arrays in order to prevent any ambiguity that can arise from the side lobes.

ACKNOWLEDGMENT

This work was partially supported by CNCISIS, PN II - HR, contract no. 13/1.10.2007. O.M. thanks European Union contract no. POSDRU/6/1.5/S/22 for the Ph.D. fellowship.

REFERENCES

- [1] B. Hatami, K. Alavi, K. Pahlavan, and M. Kanaan, "A Comparative Performance Evaluation of Indoor Geolocation Technologies," *Interdisciplinary Information Sciences*, vol. 12, no.2, p. 133-146, 2006.
- [2] K. Pahlavan, X. Li, and J. Makela, "Indoor Geolocation Science and Technology", *IEEE Communications Magazine*, vol. 40, no. 2, p. 112-118, 2002.
- [3] K. D'hoel, G. Ottoy, J.-P. Goemaere, and L. De Strycker, "Indoor Room Location Estimation," *Advances in Electrical and Computer Engineering Journal*, Vol. 8, No 2, p. 78 – 81, 2008.
- [4] K. Pahlavan, F. Akgul, M. Heidari, A. Hatami, J. Elwell, and R. Tingley, "Indoor Geolocation in the Absence of Direct Path", *IEEE Wireless Communications Magazine*, vol. 13, no. 6, p. 50-58, 2006.
- [5] H. Liu, H. Darabi, P. Banerjee, L. Jing, "Survey of Wireless Indoor Positioning Techniques and Systems," *IEEE Transactions on Systems, Man, and Cybernetics, Part C: Applications and Reviews*, Vol. 37, No. 6, p. 1067-1080, 2007.
- [6] H. J. Visser "Array and Phased Array Antenna Basics", Jon Wiley & Sons Ltd, 2005
- [7] J.L. Volakis "Antenna Engineering Handbook", McGraw-Hill Companies, 2007
- [8] M. Taguchi, K. Era, K. Tanaka "Two Element Phased Array Dipole Antenna", 22nd Annual Review of Progress in Applied Computational Electromagnetics, March 12-16, 2006